International RILEM Symposium on Concrete Modelling – CONMOD'08
26-28 May 2008, Delft, The Netherlands

DAMAGE MODEL FOR NORMAL & HIGH STRENGTH CONCRETE

Asad R. Khan [(1)], Nida Naseem [(1)]

(1) NED University of Engineering & Technology, Karachi, Pakistan

Abstract

An anisotropic damage model capable of predicting the response of normal and high strength concretes is presented in this study. The model utilizes a concrete appropriate effective compliance matrix in constructing the constitutive equations. Three parameters α, β and γ were used in the effective compliance matrix. α and β are introduced to model the different behaviour of concrete in tension and compression while the third parameter γ was introduced to account for volumetric change. The concept of multiple surfaces i.e. limit fracture surface, loading function surface and bounding surface, defined in strain-energy release space, is used to define the evolution of damage. After calibration for various strengths of concrete, ranging from 27.6 MPa to 120 MPa, the predictive capability of the proposed elasto-damage model for uniaxial and biaxial stress paths was investigated for uniaxial compression, biaxial compression, uniaxial tension and tension-compression. The simulative capability of the model to capture the phenomenological behaviour of concrete such as strain softening, stiffness degradation, biaxial strength envelope, volumetric dilatation, different behaviour in tension and compression, and gain in strength under increasing confinement is reflected. The predicted results correlate well with the available experimental data.

1. INTRODUCTION

In recent years considerable research has been focused on modelling of mechanical behaviour of concrete. The mechanical behaviour of concrete is very complicated and the possible variations in material characteristics have not been modelled effectively under various theoretical frameworks. Typical trends in concrete behaviour include: stiffness degradation, strain softening, volumetric dilatation, different behaviour in tension and compression, and gain in strength under increasing confinement.

The theory of continuum damage mechanics (CDM) has been used extensively to model the progressive degradation of the mechanical properties of materials caused by microcracking. Concrete contains numerous microcracks, even before the application of the external loads. Under applied loading, the initiation of new microcracks and the growth of existing microcracks contribute to the observed nonlinear behaviour in concrete, ultimately

causing the failure. The existence of microcracks and their propagation cause what is termed as "damage" to the concrete.

The concept of bounding surface, initially used in plasticity for metals, was applied to concrete by Suaris et al. [1], Voyiadjis and Abu-Lebdeh [2], Yazdani and Karnawat [3]. It was modified and used successfully to predict most of the essential features of normal and high strength concrete by Khan et al. [4].

The present study is aimed towards improving predictive capabilities of constitutive model for normal and high strength concrete proposed by Khan et al. [4]. This is achieved by defining critical strain energy release rate R_c as a function of initial modulus of elasticity, E_o, uniaxial compressive strength, f_c', and parameters α and β as a function of E_o, f_c', and normalized strain invariants, $\frac{I_1}{\varepsilon_3}$ & $\frac{J_2}{e_3^2}$. The constitutive relations and damage growth are derived using the approach presented by the authors in their previous work. The proposed mode is simple, captures the constitutive behaviour of concrete and can be directly implemented into a general-purpose finite element code with relative ease.

2. THEORETICAL PRELIMINARIES

2.1 Effective Compliance Matrix

Following compliance matrix as postulated by Khan et al. [4] is used in the study

$$\widetilde{C}_{11} = \frac{1}{E_o}\frac{(1-\beta\omega_1)^2}{(1-\alpha\omega_1)^2(1-\beta\omega_2)^2(1-\beta\omega_3)^2} \qquad \widetilde{C}_{22} = \frac{1}{E_o}\frac{(1-\beta\omega_2)^2}{(1-\alpha\omega_2)^2(1-\beta\omega_3)^2(1-\beta\omega_1)^2} \tag{1}$$

$$\widetilde{C}_{33} = \frac{1}{E_o}\frac{(1-\beta\omega_3)^2}{(1-\alpha\omega_3)^2(1-\beta\omega_1)^2(1-\beta\omega_2)^2}$$

$$\widetilde{C}_{12} = -\frac{\nu 1}{E_o(1-\alpha\omega_1)(1-\alpha\omega_2)(1-\beta\omega_3)^2(1-\gamma\omega_1)(1-\gamma\omega_2)} = \widetilde{C}_{21}$$

$$\widetilde{C}_{13} = -\frac{\nu 1}{E_o(1-\alpha\omega_1)(1-\alpha\omega_3)(1-\beta\omega_2)^2(1-\gamma\omega_1)(1-\gamma\omega_3)} = \widetilde{C}_{31}$$

$$\widetilde{C}_{23} = -\frac{\nu 1}{E_o(1-\alpha\omega_2)(1-\alpha\omega_3)(1-\beta\omega_1)^2(1-\gamma\omega_2)(1-\gamma\omega_3)} = \widetilde{C}_{32}$$

in which the thermodynamic constraint requirement $E_i\nu_{ji} = E_j\nu_{ij}$ has been ensured.

2.2 Bounding Surface

In order to construct a rational model accounting for damage growth, concepts are borrowed from incremental theory of plasticity in general and the bounding surface plasticity model in particular. Plasticity bounding surface models, requires definition of multiple surfaces in stress space. However, the fundamental surfaces in the present work are best described in strain-energy release space, as proposed by Suaris et al. [1].

$$f = (R_i R_i)^{1/2} - R_c / b = 0 \tag{2}$$

$$F = (\overline{R}_i \overline{R}_i)^{1/2} - R_c = 0$$

$$f_o = (R_i R_i)^{1/2} - R_o = 0$$

where, f is the loading function surface, F is the bounding surface, f_o is a limit fracture surface [3]. The loading function surface (f) is defined in terms of thermodynamic-force conjugates, R_i, where,

$$R_i = \rho \frac{\partial \Lambda}{\partial \omega_i}(\sigma_{ij}, \omega_i) \tag{3}$$

where $\rho\Lambda$ is the strain energy density and $\overline{R}_i$ is an image point on $F = 0$ associated with a given point R_i on $f = 0$ defined by a mapping rule

$$\overline{R}_i = bR_i \tag{4}$$

$$b = R_c / (R_i R_i)^{1/2}$$

with the mapping parameter b ranging from an initial value of ∞ to a limiting value of 1 on growth of loading surface to coalesce with bounding surface. R_c, critical strain energy release rate, is a parameter of the model and is calibrated to the standard uniaxial compression test, and is suggested to be a function of uniaxial compressive strength and modulus of elasticity. R_o defines the initiation of microcracking which occurs at about 40% of the peak stress as indicated by experimental results, and it varies with the compressive strength of concrete as:

$$R_o = \sqrt{2}\beta(0.4 f_c')^2 / E_o \tag{5}$$

Damage is hypothesized to accumulate at levels of strain energy release rate resulting in the loading surface (f) traversing the limit fracture surface (f_o) and rupture in the damage sense is said to occur when f grows large enough to coalesce with the bounding surface F fixed in the R_i space.

The parameters α and β in the effective compliance matrix control the movement of the loading surface which describes the onset of damage or failure, i.e. higher values of α and β means faster movement of loading surface and hence lower peak stress, as it will reach the bounding surface much earlier than with lower values of α and β. This makes the model flexible enough to accommodate normal as well as high strengths of concrete.

2.3 Damage Evolution

The damage growth is determined from the loading surface, f, as

$$d\omega_i = d\lambda \frac{\partial f}{\partial R_i} \tag{6}$$

Where $d\lambda$ is defined as

$$d\lambda = \frac{\dfrac{\partial f}{\partial R_i}\dfrac{\partial R_i}{\partial \sigma_k} d\sigma_k}{\dfrac{\partial k}{\partial \overline{\omega}_p} - \dfrac{\partial f}{\partial R_i}\dfrac{\partial R_i}{\partial \omega_j}\dfrac{\partial f}{\partial R_j}} \tag{7}$$

Introducing damage modulus $H = \dfrac{\partial k}{\partial \overline{\omega}_p}$, that can be measured experimentally in a uniaxial compression test and the same form is assumed for more general stress paths. In the present work, H is expressed as a function of the distance between the loading and the bounding surface, given by

$$H = \frac{D\delta}{\langle \delta_{in} - \delta \rangle} \tag{8}$$

where $D = 2.65$ is a constant and < > are Macaulay brackets that set the quantity within it to zero if the value is negative. The normalized distance δ between the loading and bounding surfaces is given by

$$\delta = 1 - \frac{1}{b} \tag{9}$$

$\delta = \delta_{in}$ corresponds to R_o when the loading surface first crosses the limit fracture surface.

3. INCREMENTAL STRESS STRAIN RELATIONS

The incremental stress-strain law is given by

$$d\varepsilon_i = \left\{ \widetilde{C}_{ij} + \sigma_l \frac{\partial \widetilde{C}_{ij}}{\partial \omega_k} \frac{\partial f}{\partial R_k} \frac{d\lambda}{d\sigma_l} \right\} d\sigma_j \tag{10}$$

where $d\lambda$ is defined in Equation (7). Equation (11) is useful in a stress control testing.

The incremental stress-strain law for strain control testing is given by

$$d\sigma_i = \left\{ D_{ij} + \varepsilon_l \frac{\partial D_{ij}}{\partial \omega_k} \frac{\partial f}{\partial R_k} \frac{d\lambda}{d\varepsilon_l} \right\} d\varepsilon_j \tag{11}$$

where $d\lambda$ is defined in Equation (12).

$$d\lambda = \frac{\dfrac{\partial f}{\partial R_k}\dfrac{\partial R_k}{\partial \varepsilon_j} d\varepsilon_j}{H - \dfrac{\partial f}{\partial R_k}\dfrac{\partial R_k}{\partial \omega_j}\dfrac{\partial f}{\partial R_j}} \tag{12}$$

Incremental stress-strain relationships for specific cases of uniaxial compression, uniaxial tension and equal biaxial compression can be found elsewhere [4].

4. DETERMINATION OF REGRESSION COEFFICIENTS

The parameters α, β and γ are functions of E_o, f_c', and $\frac{I_1}{\varepsilon_3}$ & $\frac{J_2}{e_3^2}$ (where $I_1 = \varepsilon_{kk}$ & $J_2 = \frac{1}{2} tr\,(e_{ij})$ where R_c is function of f_c' and E_o only. Here, ε_3 and e_3 represent the minor principal and deviatoric strain, respectively. The suggested forms of α, β and γ are as follows:

$$\alpha = \alpha_0(f_c', E_o) + \alpha_1(f_c', E_o)\frac{I_1}{\varepsilon_3} + \alpha_2(f_c', E_o)\frac{J_2}{e_3^2} + \alpha_3(f_c', E_o)\frac{I_1}{\varepsilon_3}\frac{J_2}{e_3^2} \quad (13)$$

$$\beta = \beta_0(f_c', E_o) + \beta_1(f_c', E_o)\frac{I_1}{\varepsilon_3} + \beta_2(f_c', E_o)\frac{J_2}{e_3^2} + \beta_3(f_c', E_o)\frac{I_1}{\varepsilon_3}\frac{J_2}{e_3^2}$$

$$\gamma = \gamma(f_c', E_o) \quad (\sigma 1 < 0, \sigma 2 < 0)$$

These parameters were calibrated by regressing against experimental σ–ε data for different f_c'. The range of f_c' used in regression varies from 27.6 MPa (4,000 psi) to 120 MPa (17,400 psi), and is listed in Table 1. Details of regression can be found elsewhere [6].

Final form of R_c, α_i's, β_i's and γ is as follows:

$$R_c = 8.2451\text{-}7.0843\text{E-}04\times f_c' - 6.15\text{E-}07\times E_o + 8.22324\text{E-}11\times f_c'\times E_o \quad (14)$$

- α for (σ1 > 0, σ2 < 0)

$$\alpha_0 = -3.324\text{E}+01 + 2.348\text{E-}03\times f_c' + 4.060\text{E-}06\times E_o - 3.057\text{E-}10\times E_o\times f_c' \quad (15)$$

$$\alpha_1 = -2.701\text{E}+01 + 4.589\text{E-}03\times f_c' + 1.992\text{E-}06\times E_o - 5.570\text{E-}10\times f_c'\times E_o$$

$$\alpha_2 = 5.540\text{E}+01 - 5.375\text{E}-03\times f_c' - 6.053\text{E-}06\times E_o + 6.776\text{E-}10\times f_c'\times E_o$$

$$\alpha_3 = 1.989\text{E}+01 - 2.641\text{E-}03\times f_c' - 1.845\text{E-}06\times E_o + 3.262\text{E-}10\times f_c'\times E_o$$

- α for (σ1 > 0 , σ2 ≥ 0)

$$\alpha = 26.5563 - 2.928157\text{E-}03\times f_c' - 2.5423\text{E-}06\times E_o + 3.55154\text{E-}10\times f_c'\times E_o \quad (16)$$

- α = 0 for (σ1< 0, σ2 < 0)
- β for (σ1 < 0, σ2 < 0)

$$\beta_0 = 9.9351\text{E-}01 - 6.5957\text{E-}05\times f_c' - 1.2277\text{E-}07\times E_o + 8.6393\text{E-}12\times E_o\times f_c' \quad (17)$$

$$\beta_1 = -1.5283\text{E-}01 + 1.3190\text{E-}05\times f_c' + 1.5177\text{E-}08\times E_o 1.5719\text{E-}12\times f_c'\times E_o$$

$$\beta_2 = -5.0825\text{E-}01 + 2.1187\text{E-}05\times f_c' + 7.2680\text{E-}08\times E_o - 3.2310\text{E-}12\times f_c'\times E_o$$

$$\beta_3 = 2.7165\text{E-}01 + -1.1523\text{E-}05\times f_c' - 3.8623\text{E-}08\times E_o + 1.7450\text{E-}12\times f_c'\times E_o$$

- β for ($\sigma1 > 0, \sigma2 < 0$)

$$\beta = 0.643665 - 4.69309 - 05 \times f_c' - 7.71E-08 \times E_o + 6.022E-12 \times f_c' \times E_o \quad (18)$$

- $\beta = 0$ for ($\sigma1 > 0, \sigma2 > 0$)
- γ ($\sigma1 < 0, \sigma2 < 0$)

$$\gamma = 3.1344 - 1.1826E-4 \times f_c' - 2.903E-07 \times E_o + 1.28434E-11 \times f_c' \times E_o \quad (19)$$

6. RESULTS

Predicted results are verified for uniaxial and biaxial loading conditions by comparing them with the available experimental and analytical results. A strain control program is used for plotting curves for predicted stress-strain response, volumetric dilatation and apparent Poisson's ratio for biaxial loading conditions.

Three different concretes (concrete A, f_c' = 27.6 MPa (4,000 psi), concrete B, f_c' = 65 MPa (9,434 psi) and concrete C, f_c' = 120 MPa (17,416 psi) were selected for comparison of predicted results of the model. For the case of uniaxial compression, comparison with experimental results and analytical results of Khan et al. [4] shows that the predicted curves for concretes A and B (Fig. 1) are stiffer and less ductile than the experimental curves i.e. the predicted peak stress compares quite well but the strains are somewhat on the lesser side but are softer than the analytical results of Khan et al. [4]. This can be attributed to the absence of plastic strains. Additional plastic strains will shift the curves to the right, making it comparable with the experimental values. Curve for concrete C (Fig. 1), is in close agreement with the experimental and analytical curves both in terms of peak stress and peak strain. It is evident from Figure 1 that the model can capture the increasing brittleness and decreasing ductility with the increase in uniaxial compressive strength quite effectively.

Figures 1 - 3 reflect the predictive capability of the model to capture the phenomenological behaviour of volumetric dilatation. In Figure 1, curves for lateral strains are shown in which the increase in lateral strains as the stress reaches the peak stress is clearly visible with curves from present study showing more smmothness. This increase in lateral strains is due to the dramatic increase in apparent Poisson's ratio (Figure 2), which results in the change of sign of dilatancy (volumetric strain) as shown in Figure 3. It can be seen from the figure that concrete always exhibits this phenomenon under biaxial compression irrespective of the stress paths. Figure 2 represents the change in Poisson's ratio for all the three concretes. The curves are consistent with the observed behaviour as the change in Poisson's ratio is more evident near the peak stress and are smoother than the ones predicted by Khan et al. [4].

For the case of biaxial compression, comparison with the experimental results of Kupfer et al. [7] (Figure 4) indicates that the predicted peak stress envelope is in close agreement with the experimental peak stress.

It should be noted that this improvement in results was obtained by defining R_c as a function of uniaxial compressive strength and initial modulus of elasticity. Since it is already shown that this rather simple approach is capable of capturing almost all the observed phenomenological trends of concrete, incorporation of more three dimensional data will yield a more rigorous model capable of predicting multiaxial behaviour of concrete.

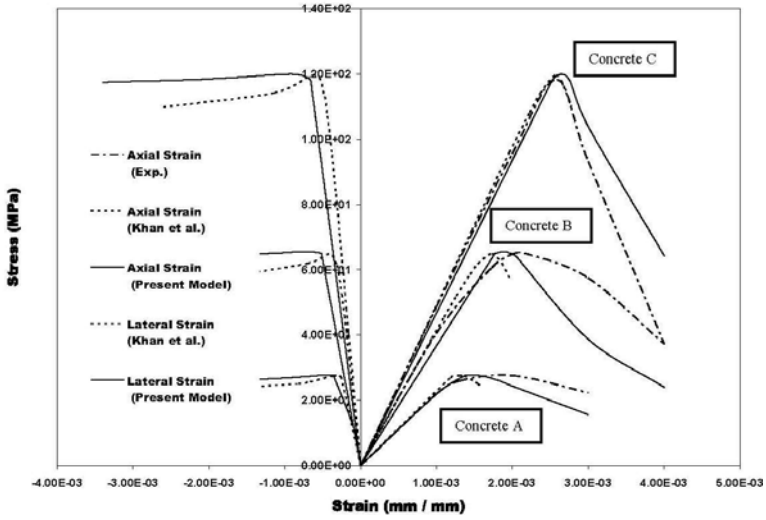

Figure 1: Stress-strain curves for uniaxial compression

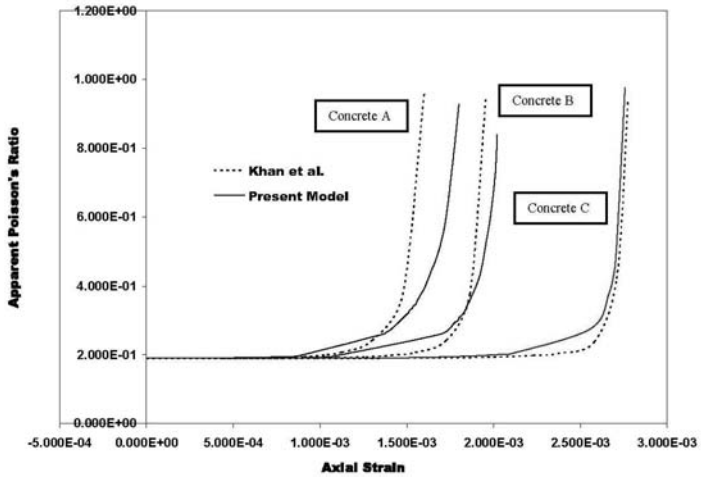

Figure 2: Apparent Poisson's Ratio under uniaxial compression

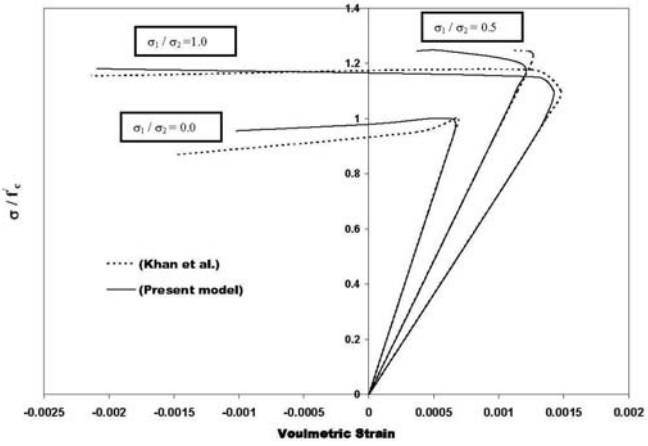

Figure 3: Volumetric dilatation of concrete under biaxial compression

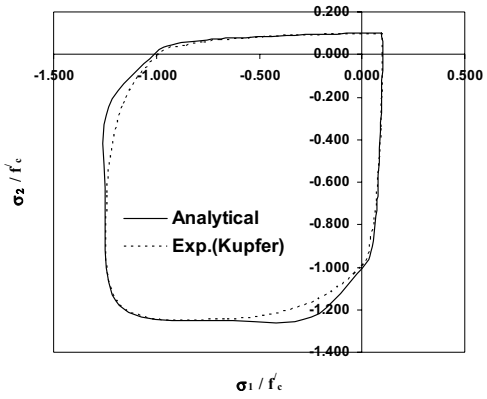

Figure 4: Biaxial strength interaction curve for concrete

7. CONCLUSIONS

- An elasto-damage bounding surface model developed by Khan et al. [4] for monotonic behaviour of normal and high strength concrete is improved in this paper. A generalized compliance matrix in the principal coordinate system proposed by Khan et al. [4] is used. Critical strain energy release rate R_c is defined as a function of elastic modulus and uniaxial compressive strength which improved overall performance of the model.
- Results presented in the paper demonstrate that the present model predicts the behaviour of concrete under biaxial monotonic loadings adequately and captures almost all the essential features of concrete including the volumetric dilatation.
- In order to make the model general and applicable to real three dimensional problems, work is in progress and more triaxial data will be incorporated in determining the regression coefficients.

ACKNOWLEDGEMENTS

The authors are indebted to the Department of Civil Engineering at NED University of Engineering & Technology, Karachi, Pakistan and the University itself, in the pursuit of this work.

REFERENCES

[1] Suaris, W., Onyang, C. and Fernando, V.M., 'Damage model for cyclic loading of concrete', *J. Engg. Mech. ASCE* **116** (5) (1990) 1020-1035.
[2] Voyiadjis, G.Z. and Abu-Lebdeh, T.M., 'Damage model for concrete using bounding surface concept', *J. Engg. Mech. ASCE* **119** (9) (1993) 1865-1885.
[3] Yazdani, S. and Karnawat, S., 'A constitutive theory for brittle solids with application to concrete', *Int. J. Damage Mech.* **5** (1) (1996) 93-110.
[4] Khan, A.R., Al-Gadhib, A.H. and Baluch, M.H., 'Three Parameters Damage Model for Concrete', in Proceedings of the Fifth International Conference on Computational Structures Technology, Leuven, Belgium, 2000 95–106.
[5] Kupfer, H., Hilsdorf, H.K. and Rusch, H., 'Behavior of concrete under biaxial stresses', *ACI Journal Proceedings* **66** (8) (1969) 656-666.